Excitonic Bloch oscillations in a terahertz field

M. M. Dignam
Department of Physics, Lakehead University, Thunder Bay, Ontario, Canada P7B 5E1
(Received 29 June 1998)

We present a formalism for calculating the coherent response of a semiconductor superlattice in combined static and terahertz along-axis electric fields. The method is based upon the semiconductor Bloch equations in a basis of single-particle Wannier-Stark ladder states. We employ this formalism to calculate, for the first time, the short-pulse absorption spectrum of excitons in a superlattice in combined static and terahertz electric fields. We find that for terahertz fields with frequencies much less than the Bloch oscillation frequency, the absorption peaks are shifted by approximately $eF(t_o)nd$, where d is the superlattice period, n is the Wannier-Stark ladder index of the peak, and $F(t_o)$ is the value of the terahertz field at the time when the optical pulse reaches the sample. For terahertz fields with frequencies near the Bloch oscillation frequency, the shifts are qualitatively similar, but of the opposite sign and are generated via mixing of the optical and terahertz frequencies. [S0163-1829(99)08807-4]

I. INTRODUCTION

Coherent effects in photoexcited semiconductor superlattices and quantum wells have received considerable attention in recent years. Some important examples include beating of light and heavy holes in quantum wells,[1] wave-packet oscillations in coupled-double-quantum wells,[2] and Bloch oscillations (BO's).[3] All of these examples involve the creation of excitons using ultrashort optical pulses near the band gap. The evolution of the resulting excitonic states has been probed experimentally via degenerate four wave mixing (DFWM), pump-probe spectroscopy, and the detection of terahertz radiation. Such experiments provide information on dephasing times and mechanisms, the effects of external fields, and the nature of nonlinear processes in semiconductor nanostructures.

There has been a relatively large number of theoretical treatments of these systems in recent years. The most common approach has been the application of the semiconductor Bloch equations (SBE's).[4–9] Other approaches range from phenomenological two- and three-level models[2] to the more complete dynamically controlled truncation (DCT) technique[10,11] and the quasibosonic treatment of Hawton and Nelson.[12] The challenge lies in developing a description of these potentially complex systems which treats electron-electron interactions in a satisfactory manner, while remaining computationally tractable.

The problem we are considering in this work is the optical response of a semiconductor superlattice in applied along-axis static and terahertz electric fields. In the absence of the terahertz field, the eigenstates of this system are the excitonic Wannier-Stark ladder (WSL) states. These were first detected experimentally by Mendez, Agulló-Rueda, and Hong,[13] and have also been treated theoretically by a number of authors.[5,6,14–16] If this system is excited via an ultrashort ($\sim$100 fs) optical pulse near the band gap, excitonic Bloch oscillations result. Bloch oscillations have been a topic of interest and controversy for a long time.[17] They were first detected unambiguously by Feldmann *et al.*[3] using DFWM and by Waschke *et al.*[18] by directly measuring the terahertz radiation resulting from the oscillating excitonic dipole. This system has also been studied theoretically by a number of authors. The models developed vary rather widely in their approach. A number of theories neglect the Coulomb interaction but include all the excited states.[19–21] There have also been several excitonic theories. Some of these have included excited excitonic states but have employed a simplified contact potential for the electron-hole Coulomb interaction;[6,7] some have employed the full Coulomb interaction but only included $1s$ excitons;[15,22,23] and some have included the full Coulomb interaction and the excitonic states with in-plane excitation.[5,8]

A related system that has been studied theoretically by a number of authors is a semiconductor superlattice in an applied terahertz field alone, with no static electric field. The linear optical absorption of such a system was recently investigated by Johnsen and Jauho[24] without the inclusion of excitonic effects, and by Meier and co-workers[7–9] with excitonic effects included. These systems produce the extremely interesting feature of dynamic localization, which dramatically alters the linear optical response of the system.

In this work, we consider a system in which *both static and terahertz along-axis fields are applied*. Thus far there have been no theoretical results presented of the excitonic states in a semiconductor superlattices in such a system. A related system has been modeled by Meier *et al.*[6,7,9] where the DFWM signals in a superlattice in a static electric field were calculated. In such a system, the carriers generated by the pump pulse undergo Bloch oscillations. These oscillating carriers generate terahertz fields that in turn interact with the carriers. Thus, this system is related to the WSL in the presence of a terahertz field, but is clearly more complicated in that there are electron correlations not captured by a simple along-axis terahertz field. In that work, however, no calculation of the spectrally resolved DFWM signal was presented.

The central results of the work presented here are that when an along-axis terahertz field is applied to a superlattice in static electric field, it produces time-dependent shifts of the WSL absorption peaks; that these peak shifts are due to nonlinear mixing of the optical and terahertz fields; and that

these peak shifts are qualitatively unchanged when excitonic effects are included.

This work is partially motivated by the recent work by Sudzius *et al.*[22] and Lyssenko *et al.*,[23] in which the spectrally resolved DFWM signal from a superlattice in a static electric field revealed that the peaks associated with the excitonic WSL states shift in energy as the pump-probe time delay time τ_{pp} is changed. Moreover, this shift is proportional to the pump intensity and oscillates approximately as $\cos(\omega_B\tau_{pp}+\theta)$, where $\omega_B=eF_od/\hbar$ is the BO frequency, d is the superlattice period, and F_o is the static along-axis electric field. The interpretation of this result was that the pump pulse generates a Bloch-oscillating excitonic wave packet, which produces an along-axis terahertz field. This field then acts as an adiabatic addition to the static electric field and shifts the excitonic energy levels (and hence the absorption peaks) to energies given by $E_n=E_0+e(F_o+F(t_o))nd$, where $F(t_o)$ is the value of the generated terahertz field when the probe pulse reaches the sample and n is the WSL index of the state. We shall refer to this model as the *quasistatic* model. To date there has been no theoretical treatment of this system that explains the peak shifts including the dynamical response to the self-generated terahertz field.

In this work, we present the results of a calculation of the optical response of a semiconductor superlattice in applied along-axis static and terahertz electric fields to an ultrashort ($\sim$100 fs) optical pulse. The method is based upon a form of the SBE's in which a basis of noninteracting electron and hole WSL states are employed rather than the usual k_z states. A similar approach has been used previously by Hader *et al.*[5] for a system with only a static electric field. We apply this basis to a system with applied static and terahertz fields. This basis has the advantage that it makes transparent the nature of coupling between the different WSL states via the terahertz field. We use this technique to calculate the linear absorption spectrum as a function of the terahertz field frequency and phase. This calculation is of interest because it is just now becoming possible to study the effects of terahertz fields on semiconductor nanostructures. In addition, the calculation also has some relevance to pump-probe and DFWM experiments on superlattices in static electric fields, for in these systems a terahertz field arises from the Bloch-oscillating carriers generated by the pump pulse. Clearly it is a great simplification to claim that these systems can be adequately described by including only a spatially homogeneous along-axis terahertz field. In fact it has been demonstrated that exciton-exciton correlations can play an important role in determining the DFWM signal.[25] However, the results do reproduce qualitatively the experimentally-observed peak shifts in DFWM experiments and thus seem to capture the mean-field effect of the oscillating charges on the excitonic states.

We find that for terahertz field frequencies that are less than the inverse of the interband dephasing time, the terahertz field produces a frequency shift of the absorption peaks that is in agreement with the quasistatic picture, but with a shift amplitude that decreases as the terahertz frequency increases. We also observe that there are also significant shifts of the peaks when the terahertz frequency is close to the BO frequency. These shifts *cannot* be understood via the quasistatic model discussed above, but are best understood as the result of sum and difference mixing of the optical and terahertz frequencies. Finally, we find that results for the *excitonic* case are qualitatively similar to those found in a simplified noninteracting electron-hole model as long as the static electric fields are large enough such that the excitonic binding energies are considerably less than the energy spacings in the Wannier-Stark ladder.

The paper is organized as follows. Section II contains the theory: in Sec. II A we present the Hamiltonian in the WSL basis; in Sec. II B the equations describing the dynamics of the reduced density matrices are developed; and finally, in Sec. II C we present the expression for the polarization and optical absorption coefficient. In Sec. III A we present the results in the single-particle or noninteracting approximation, where the Coulomb interaction between the electrons and holes is neglected. Then, in Sec. III B we present the results for 1s-like excitons using the full electron-hole Coulomb interaction. Finally in Sec. IV we summarize the results and their implications.

II. THEORY

In this section, we develop the equations of motion describing the coherent dynamics of excitons in a semiconductor superlattice in the presence of a time-dependent electric field applied along the growth axis z. We then use these equations to develop the expression for the absorption of an ultrashort optical pulse near the band gap. The development is similar to that of the usual SBE's except that we employ as our basis the single-particle one-band WSL states, rather than the k_z-state basis that is usually employed. As mentioned above, a similar approach has been used previously by Hader *et al.*[5] for a system with only a static electric field. In this work, however, we apply this basis to a system with applied static *and terahertz fields*. For this system, this basis explicitly shows clearly the way in which the terahertz couples the different WSL levels, and thus makes the basic physical effect of the terahertz field essentially transparent. There are two further advantages of this method over the usual SBE's in the k_z-state basis. First, the noninteracting WSL basis is much closer to the actual excitonic basis in the presence of the static electric field and thus the physical significance of terms is much more transparent. Second, the electrons and holes are spatially localized in the z direction in the WSL basis, and the only states that are optically excited are those with an appreciable electron-hole overlap integral. Therefore, we need only include WSL states in our basis for which the electron-hole overlap is significant. This makes truncation of the basis simple, and allows for a relatively small basis. In contrast, in the k_z-state basis, states of all along-axis $\mathbf{k}$ vectors k_z must be included on a relatively dense grid, resulting in a larger basis.[26] This difference between the bases has been discussed in earlier works in a somewhat different context.[5,14] We begin by presenting the Hamiltonian for the system. We then discuss the dynamical equations for the density matrix elements, and finish the section by presenting the expression for the optical absorption spectrum.

A. Hamiltonian

We work within the envelope function approximation and neglect band nonparabolicities and valence-band mixing.

Furthermore, we limit ourselves to the inclusion of only the first superlattice minibands from both the conduction and valence bands. Within the one-miniband approximation, it has been shown[27] the eigenstates for noninteracting electrons in a static electric field F_o are spatially localized in the z direction and have equal energy spacings of $eF_o d$, where d is the period of the superlattice. The wave functions for the conduction-band and valence-band electrons in a static along-axis electric field can thus be written as

$$\psi_n^{c,v}(\mathbf{r},\mathbf{k}) = \frac{1}{\sqrt{A}} e^{i\mathbf{k}\cdot\boldsymbol{\rho}} \chi_n^{c,v}(z) u_o^{c,v}(\mathbf{r}), \tag{1}$$

where c (v) refers to conduction- (valence-) band electrons, $\mathbf{r}$ is a three-dimensional position vector, ρ is the corresponding two-dimensional position vector in the (x,y) plane, $\mathbf{k}$ is the two-dimensional in-plane wave vector, A is the in-plane normalization area, and the $u_o^{c,v}(\mathbf{r})$ are the periodic portions of the bulk Bloch functions at the conduction- and valence-band extrema, respectively (assumed to be the same for both materials in the superlattice). The functions, $\chi_n^{c,v}(z) = \chi_n^{e,h}(z)$, are so-called WSL states, which are the eigenstates of the one-dimensional Hamiltonians,

$$H^{e,h}(z) = \frac{\partial}{\partial z} \frac{-\hbar^2}{2m_z^{e,h}(z)} \frac{\partial}{\partial z} + U^{e,h}(z) - q_{e,h} F_o z, \tag{2}$$

in the single-miniband approximation, where $m_z^{e,h}(z)$ is the layer-dependent along-axis effective mass for the electrons or holes, $U^{e,h}(z)$ is the superlattice potential experienced by the electrons or holes due to band-gap discontinuities [with $U^{e,h}(z)=0$ in the wells], $q_e=-e$ and $q_h=e$ are the charges of the electrons and holes, respectively, and e is the modulus of the charge on an electron. Within the one-miniband approximation, these WSL eigenstates can be expanded in the basis of miniband Wannier states $a^\lambda(z)$ localized at different sites:

$$\chi_n^e(z) = \sum_m C_{m-n}^e a^c(z-md), \tag{3}$$

$$\chi_n^h(z) = \sum_m C_{m-n}^h a^v(z-md). \tag{4}$$

In the nearest-neighbor tight-binding approximation, the WSL states in Eqs. (3) and (4) are replaced by single-site ground states and one finds that $C_{m-n}^{e,h} = J_{m-n}(\theta_{e,h})$, where $J_m(\theta)$ is a Bessel function of the first kind of order m and $\theta_{e,h} \equiv \Delta_{e,h}/2q_{e,h}F_o d$, where $\Delta_{e,h}$ is the bandwidth of the electron or hole miniband.[27] In the following development we take the general case and do *not* assume the more restrictive tight-binding result.

The full Hamiltonian for the system within the two-band basis is

$$H = H_o + H_T + H_I + H_C, \tag{5}$$

where H_o is the Hamiltonian in the absence of Coulomb interactions, the terahertz field, and the external optical field (but including the static electric field) and is given by

$$H_o = \sum_{\mathbf{k}} \sum_n [E_{n,\mathbf{k}}^e \alpha_{n,\mathbf{k}}^\dagger \alpha_{n,\mathbf{k}} + E_{n,\mathbf{k}}^h \beta_{n,\mathbf{k}}^\dagger \beta_{n,\mathbf{k}}], \tag{6}$$

where $E_{n,\mathbf{k}}^e$ and $E_{n,\mathbf{k}}^h$ are the single-particle energies for the electrons and holes, $\alpha_{n,\mathbf{k}}^\dagger$ and $\alpha_{n,\mathbf{k}}$ ($\beta_{n,\mathbf{k}}^\dagger$ and $\beta_{n,\mathbf{k}}$) are the creation and annihilation operators, respectively, for an electron (hole) in the WSL state with index n and in-plane wave vector $\mathbf{k}$. The single-particle WSL energies for electrons and holes are given, respectively, by

$$E_{n,\mathbf{k}}^e = E_{gap} + \frac{\hbar^2 \mathbf{k}^2}{2m_\parallel^e(z)} + E_0^e + eF_o nd \tag{7}$$

and

$$E_{n,\mathbf{k}}^h = \frac{\hbar^2 \mathbf{k}^2}{2m_\parallel^h(z)} + E_0^h - eF_o nd, \tag{8}$$

where E_{gap} is the band gap of the bulk semiconductor in the wells, n is an integer, and $E_0^{e,h}$ are the $n=0$ eigenenergies of the one-dimensional single-particle Hamiltonians $H^{e,h}(z)$ of Eq. (2). In general these energies will depend upon the electric field due to the quantum-confined (QC) Stark effect, but if the WSL state is expanded in terms of the Wannier states of the zero-field Hamiltonian, they are field independent.

The second term in H, H_T, contains the interaction with the terahertz field, $F(t)$, and is given by

$$\begin{aligned} H_T = {} & eF(t) \sum_{\mathbf{k}} \sum_n [(nd + Z_0^c) \alpha_{n,\mathbf{k}}^\dagger \alpha_{n,\mathbf{k}} - (nd + Z_0^v) \beta_{n,\mathbf{k}}^\dagger \beta_{n,\mathbf{k}}] \\ & + eF(t) Z_0^v N^v - \frac{F(t)}{F_o} \sum_{\mathbf{k}} \sum_n \sum_{p\neq 0} [(\varepsilon_p^e - eF_o Z_p^c) \\ & \times \alpha_{n,\mathbf{k}}^\dagger \alpha_{n-p,\mathbf{k}} + (\varepsilon_p^h + eF_o Z_{-p}^v) \beta_{n,\mathbf{k}}^\dagger \beta_{n-p,\mathbf{k}}], \end{aligned} \tag{9}$$

where F_o is the along-axis static electric field and

$$Z_p^\lambda \equiv \int dz a^{\lambda *}(z-pd) z a^\lambda(z) \tag{10}$$

is the matrix element of z between Wannier states at sites p and 0. The integer N^v gives the total number of states in the first valence miniband (in three dimensions), and

$$\varepsilon_p^{e,h} \equiv \frac{1}{N_z} \sum_{k_z} \epsilon^{e,h}(k_z) e^{ik_z pd} \tag{11}$$

is the pth Fourier component of the along-axis energy dispersion, $\epsilon^{e,h}(k_z)$, for the electron or hole miniband when $F_o=0$. In deriving this result, the interband transitions due to the terahertz field have been neglected (as they are energetically very unfavorable) and we have used the summation relations for the C_n^e found in the Appendix. In general the Z_p^λ are expected to be very small (particularly for $p\neq 0$) due to the orthogonality of the Wannier states. In particular, if the superlattice potential has inversion symmetry about the well centers, then $Z_p^\lambda = 0$ rigorously. If one uses a nearest-neighbor tight-binding basis, using the ground state of the *biased* wells to approximate the Wannier functions,[14] then Z_0^c and Z_0^v are the only nonzero elements, and these elements simply give the displacement of the well states, which leads

to the QC Stark shift of the levels. In the remainder of the paper we shall only consider superlattices with inversion symmetry where it is rigorously true that $Z_p^{\lambda}=0$.

The term H_I in Eq. (5) contains the interaction with the optical field. If we write the optical field in the form

$$\boldsymbol{\mathcal{E}}(\mathbf{r},t)=\boldsymbol{\mathcal{E}}_o(t)e^{i\boldsymbol{\kappa}\cdot r}+\text{c.c.}, \tag{12}$$

where $\boldsymbol{\kappa}$ is the photon wave vector, then H_I is given in the dipole approximation by

$$H_I=\sum_{\mathbf{k}}\sum_{n,p}\boldsymbol{\mathcal{E}}_o(t)\cdot[\mathbf{d}_p^{cv}\alpha_{n,\mathbf{k}}^{\dagger}\beta_{n+p,-\mathbf{k}}^{\dagger}+\text{H.c.}], \tag{13}$$

where

$$\mathbf{d}_p^{cv}=\mathbf{M}_o\int dz\,\chi_0^{e*}(z)\chi_p^h(z), \tag{14}$$

and $\mathbf{M}_o$ is the bulk dipole matrix element. In deriving H_I we have neglected the weak $\mathbf{k}$ and p dependence of $\mathbf{M}_o$ near the band gap, as is commonly done.

The final term in the Hamiltonian is the carrier-carrier interaction term H_c, which is given by

$$\begin{aligned}H_c=\frac{1}{2}\sum_{n_1,n_2,n_3,n_4}\sum_{\mathbf{k}_1,\mathbf{k}_2}\sum_{\mathbf{q}\neq 0}\{&W^{cc}_{n_1,n_2,n_3,n_4}(\mathbf{q})\\&\times\alpha^{\dagger}_{n_1,\mathbf{k}_1+\mathbf{q}}\alpha^{\dagger}_{n_2,\mathbf{k}_2-\mathbf{q}}\alpha_{n_3,\mathbf{k}_2}\alpha_{n_4,\mathbf{k}_1}\\&+W^{vv}_{n_1,n_2,n_3,n_4}(\mathbf{q})\beta^{\dagger}_{n_3,\mathbf{k}_1+\mathbf{q}}\beta^{\dagger}_{n_4,\mathbf{k}_2-\mathbf{q}}\beta_{n_1,\mathbf{k}_2}\beta_{n_2,\mathbf{k}_1}\\&-2W^{cv}_{n_1,n_2,n_3,n_4}(\mathbf{q})\alpha^{\dagger}_{n_1,\mathbf{k}_1+\mathbf{q}}\beta^{\dagger}_{n_3,\mathbf{k}_2-\mathbf{q}}\beta_{n_2,\mathbf{k}_2}\alpha_{n_4,\mathbf{k}_1}\},\end{aligned} \tag{15}$$

where

$$\begin{aligned}W^{\lambda\lambda'}_{n_1,n_2,n_3,n_4}(\mathbf{q})\equiv\frac{2\pi e^2}{\epsilon A|\mathbf{q}|}\int dz\int dz'\,e^{-|\mathbf{q}||z-z'|}\\\times\chi^{\lambda}_{n_1}{}^{*}(z)\chi^{\lambda'}_{n_2}{}^{*}(z')\chi^{\lambda'}_{n_3}(z')\chi^{\lambda}_{n_4}(z),\end{aligned} \tag{16}$$

where ϵ is the static dielectric constant and $\mathbf{q}$ is an in-plane wave vector. In deriving Eq. (15) we have neglected the interband exchange interaction as is usually done.

B. Dynamics

We now describe the dynamics of the system by determining the equations of motion for the single-particle density matrices. There are two types of density matrices: intraband and interband. The intraband density matrices are given by

$$f^e(m_1,m_2,\mathbf{k})\equiv\langle\alpha^{\dagger}_{m_1,\mathbf{k}}\alpha_{m_2,\mathbf{k}}\rangle \tag{17}$$

for electrons and

$$f^h(m_1,m_2,\mathbf{k})\equiv\langle\beta^{\dagger}_{m_1,-\mathbf{k}}\beta_{m_2,-\mathbf{k}}\rangle \tag{18}$$

for holes. The interband density matrices given by

$$P(m_1,m_2,\mathbf{k})\equiv\langle\beta_{m_1,-\mathbf{k}}\alpha_{m_2,\mathbf{k}}\rangle. \tag{19}$$

These density matrices are diagonal in $\mathbf{k}$ but are not diagonal in the Wannier-Stark ladder indices, m_i. By looking at the effects of translation along the z axis, it can be shown that as long as the optical pulse and terahertz field are assumed to excite the sample uniformly then $f^e(m_1,m_2,\mathbf{k})$, $f^h(m_1,m_2,\mathbf{k})$, and $P(m_1,m_2,\mathbf{k})$ only depend upon the difference $m=m_2-m_1$.[28] We thus only need consider the density matrices defined by

$$f^e_m(\mathbf{k})\equiv\langle\alpha^{\dagger}_{0,\mathbf{k}}\alpha_{m,\mathbf{k}}\rangle, \tag{20}$$

$$f^h_m(\mathbf{k})\equiv\langle\beta^{\dagger}_{0,-\mathbf{k}}\beta_{m,-\mathbf{k}}\rangle, \tag{21}$$

and

$$P_m(\mathbf{k})\equiv\langle\beta_{0,-\mathbf{k}}\alpha_{m,\mathbf{k}}\rangle. \tag{22}$$

The intraband elements with $m=0$ give the population of the WSL states with in-plane wave vector $\mathbf{k}$, averaged over all WSL states in the given miniband (see Appendix). The intraband elements with $m\neq 0$ give the coherence between the different WSL states, and hence are directly related to the intraband polarization as we shall show later. The interband elements with index m, on the other hand, give the contribution to the interband polarization of electron hole pairs with WSL states that are spatially separated by md.

Straightforward operator algebra, in conjunction with the usual factoring approximation for four-operator terms,[4] yields the equations of motion for the above three density matrices in the Hartree-Fock approximation. The equation for the interband density-matrix elements is

$$\begin{aligned}i\hbar\frac{dP_m(\mathbf{k})}{dt}=&[E^e_{0,\mathbf{k}}+E^h_{0,\mathbf{k}}+e(F_o+F(t))md-i\hbar/T_2]P_m(\mathbf{k})\\&-\frac{F(t)}{F_o}\sum_{p\neq 0}[\varepsilon^e_p+\varepsilon^h_{-p}]P_{m-p}(\mathbf{k})\\&-\boldsymbol{\mathcal{E}}_o(t)\cdot\left\{\sum_p\mathbf{d}^{cv}_{p-m}[f^e_p(\mathbf{k})+f^h_{-p}(\mathbf{k})]-\mathbf{d}^{cv}_{-m}\right\}\\&-\sum_{m_1}\sum_{\mathbf{q}\neq\mathbf{0}}V^{cv}_{m,m_1}(\mathbf{q})P_{m_1}(\mathbf{k}-\mathbf{q})\\&+\sum_{m_1,m_2}\sum_{\mathbf{q}\neq\mathbf{0}}V^{cv}_{m_2,m_1}(\mathbf{q})\\&\times[f^e_{m-m_2}(\mathbf{k})+f^h_{m_2-m}(\mathbf{k})]P_{m_1}(\mathbf{k}-\mathbf{q})\\&-\sum_{m_1,m_2}\sum_{\mathbf{q}\neq\mathbf{0}}[V^{cc}_{m_1,m_2}(\mathbf{q})f^e_{m_2}(\mathbf{k}-\mathbf{q})\\&+V^{vv}_{m_1,m_2}(\mathbf{q})f^h_{-m_2}(\mathbf{k}-\mathbf{q})]P_{m-m_1}(\mathbf{k}),\end{aligned} \tag{23}$$

where

$$V^{\lambda\lambda'}_{m,m_1}(\mathbf{q})\equiv\sum_{m_3}W^{\lambda\lambda'}_{m,m_3-m_1,0,m_3}(\mathbf{q}), \tag{24}$$

T_2 is the phenomenological interband dephasing time, and we have used a number of the symmetry properties of the Coulomb matrix elements. We have used the simple single-time-constant approach hear to simplify the calculations and

simplify the discussion of the results. Although it would be preferable to employ more sophisticated approaches as has been done in other work,[5,8] this is not expected to qualitatively change the results presented here. The physical content of each of the terms in Eq. (23) is relatively simple to see. The quantities multiplying $P_m(\mathbf{k})$ in the first term form the time-dependent energy of noninteracting (NI) electron hole pairs. The second term, proportional to $F(t)/F_o$, contains the coupling between different NI WSL states due to the terahertz field. One can see from this term that the terahertz coupling of WSL states which are p levels apart is proportional to the pth Fourier component of the miniband dispersion. Hence, in a nearest-neighbor tight-binding model only neighboring levels are coupled by the terahertz field. The third term, proportional to $\mathcal{E}_o(t)$, contains the interaction with the optical field, including phase-space filling in the usual way. The fourth term contains the usual electron-hole interaction within each exciton. The fifth term contains a renormalization of the electron-hole interaction due to the presence of other excitons. And finally, the last term contains the Coulomb interaction between the excitons and the oscillating charge density that arises from the excitonic wave packets.

It is easy to see that this last term is similar in form to the terahertz-field terms. Thus, in a simplified picture, the effect of the oscillating charge density on the interband polarization can be thought of as being analogous to the effects of an along-axis terahertz field. It is tempting to think of the corresponding field as being the one generated by the oscillating dipole. A closer inspection of the two terms shows that the terms are not identical in form. In particular in the Coulomb term, there is no m dependence in the factor multiplying each $P_{m-m_1}(\mathbf{k})$. Rather, there is a $\mathbf{k}$ dependence that is not found in the terahertz terms, reflecting the in-plane spatial fluctuations of the excitonic density. Therefore the picture of the Bloch oscillating charge density generating a terahertz field that interacts with the excitons to produce the energy shifts appears to be only an approximate picture. It should, however, be at least qualitatively correct given that it is well known that the Bloch-oscillating carriers are producing a terahertz field.[18,29]

For the intraband elements we have

$$i\hbar\frac{df^e_m(\mathbf{k})}{dt}=\{e(F_o+F(t))md-i\hbar/T_1\}f^e_m(\mathbf{k}) + \boldsymbol{\mathcal{E}}_o(t)\cdot\sum_p\,[\mathbf{d}^{cv}_{-m-p}P^*_p(\mathbf{k})-\mathbf{d}^{cv*}_{m-p}P_p(\mathbf{k})] + \sum_{m_1,m_2}\sum_{\mathbf{q}\neq\mathbf{0}}V^{cv}_{m_2,m_1}(\mathbf{q})[P_{m_2+m}(\mathbf{k})P^*_{m_1}(\mathbf{k}-\mathbf{q}) - P^*_{m_2-m}(\mathbf{k})P_{m_1}(\mathbf{k}-\mathbf{q})] \tag{25}$$

and

$$i\hbar\frac{df^h_m(\mathbf{k})}{dt}=\{-e(F_o+F(t))md-i\hbar/T_1\}f^h_m(\mathbf{k}) + \boldsymbol{\mathcal{E}}_o(t)\cdot\sum_p\,[\mathbf{d}^{cv}_{m-p}P^*_p(\mathbf{k})-\mathbf{d}^{cv*}_{-m-p}P_p(\mathbf{k})] + \sum_{m_1,m_2}\sum_{\mathbf{q}\neq\mathbf{0}}V^{cv}_{m_2,m_1}(\mathbf{q})[P_{m_2-m}(\mathbf{k})P^*_{m_1}(\mathbf{k}-\mathbf{q}) - P^*_{m_2+m}(\mathbf{k})P_{m_1}(\mathbf{k}-\mathbf{q})], \tag{26}$$

where T_1 is the phenomenological intraband dephasing time, which is assumed to be the same for all intraband elements.[30] From these equations it is easy to see that at zero temperature, if there are no electrons or holes present before the optical pulse arrives then the relation between the two intraband elements is simply $f^h_m(\mathbf{k})=f^e_{-m}(\mathbf{k})$. This can be used in Eq. (23) to simplify the equation for $P_m(\mathbf{k})$.

The three equations (23), (25), and (26) are the basic equations that we use to describe coherent excitation of excitons in a superlattice in a time-dependent electric field. In this paper we shall restrict ourselves to the description of the linear response to an optical field in the presence of a static electric field and a terahertz field. In this situation, the equation for the response, $P_m(\mathbf{k})$, to first order in the optical field is

$$i\hbar\frac{dP^{(1)}_m(\mathbf{k})}{dt}=[E^e_{0,\mathbf{k}}+E^h_{0,\mathbf{k}}+e(F_o+F(t))md-i\hbar/T_2]P^{(1)}_m(\mathbf{k}) - \frac{F(t)}{F_o}\sum_{p\neq0}\,[\varepsilon^e_p+\varepsilon^h_{-p}]P^{(1)}_{m-p}(\mathbf{k}) + \boldsymbol{\mathcal{E}}_o(t)\cdot\mathbf{d}^{cv}_{-m}-\sum_{m_1}\sum_{\mathbf{q}\neq\mathbf{0}}V^{cv}_{m,m_1}(\mathbf{q})P^{(1)}_{m_1}(\mathbf{k}-\mathbf{q}). \tag{27}$$

The lowest-order intraband response is of second order in the optical field and is still given by Eqs. (25) and (26) but with $P_m(\mathbf{k})$ replaced by $P^{(1)}_m(\mathbf{k})$.

To solve Eq. (27) we expand $P^{(1)}_m(\mathbf{k})$ in the basis of the solutions, $\psi^\mu_m(\mathbf{k})$, to the eigenvalue equation

$$\hbar\omega_\mu\psi^\mu_m(\mathbf{k})=[E^e_{0,\mathbf{k}}+E^h_{0,\mathbf{k}}+eF_o md]\psi^\mu_m(\mathbf{k}) - \sum_{m_1}\sum_{\mathbf{q}\neq\mathbf{0}}V^{cv}_{m,m_1}(\mathbf{q})\psi^\mu_{m_1}(\mathbf{k}-\mathbf{q}), \tag{28}$$

which is the exciton eigenvalue equation in the absence of external fields, where the subscript μ labels the eigenstate and $\hbar\omega_\mu$ is the exciton energy. Because we are only interested in the optically accessible states, and the center-of-mass wave vector is a conserved quantity (in the Hartree-Fock approximation), we only include excitonic states with zero center-of-mass wave vector. These excitonic states are related to the corresponding configuration space exciton envelope functions by

$$\psi^\mu(z_e,z_h,\boldsymbol{\rho})=\frac{1}{\sqrt{N_zA}}\sum_{m,n}\sum_{\mathbf{k}}\,\psi^\mu_m(\mathbf{k})e^{-i\mathbf{k}\cdot\boldsymbol{\rho}}\chi^e_{n+m}(z_e)\chi^h_n(z_h), \tag{29}$$

where N_z is the number of superlattice periods. Using these excitonic states, we expand $P^{(1)}_m(\mathbf{k})$ as

$$P^{(1)}_m(\mathbf{k})=\sqrt{A}\sum_\mu\,D_\mu(t)\psi^\mu_m(\mathbf{k})e^{-i\omega_\mu t}, \tag{30}$$

where the $D_\mu(t)$ are the time-dependent expansion coefficients. Using this expansion in Eq. (27) and employing Eq. (28) we obtain

$$i\hbar\frac{dD_\nu}{dt}=-\frac{i\hbar}{T_2}D_\nu+\boldsymbol{\mathcal{E}}_o(t)\cdot\frac{e^{i\omega_\nu t}}{\sqrt{A}}\sum_m \mathbf{d}^{cv}_{-m}\sum_{\mathbf{k}} \psi^{\nu *}_m(\mathbf{k})$$
$$+eF(t)d\sum_\mu D_\mu e^{-i(\omega_\mu-\omega_\nu)t}$$
$$\times\sum_m m\sum_{\mathbf{k}} \psi^{\nu *}_m(\mathbf{k})\psi^{\mu}_m(\mathbf{k})$$
$$-\frac{F(t)}{F_o}\sum_{p\neq 0}[\varepsilon^e_p+\varepsilon^h_{-p}]\sum_\mu D_\mu e^{-i(\omega_\mu-\omega_\nu)t}$$
$$\times\sum_m\sum_{\mathbf{k}} \psi^{\nu *}_m(\mathbf{k})\psi^{\mu}_{m-p}(\mathbf{k}). \tag{31}$$

In order to proceed further we must have the solutions, $\psi^\mu(z_e,z_h,\rho)$, to the configuration-space exciton eigenvalue equation. These states and their energies have been calculated by Dignam and Sipe[14,31] by expanding them in a basis of *two-well exciton states*. In that work, only the excitonic states with $1s$-like motion,[14] or at most the first few states with excited in-plane motion[31] were calculated. In principle, however, this method can be used to calculate as many of the in-plane-excited states as is desired. We employ this method and expand the configuration-space exciton wave function in a tight-binding basis of two-well exciton states as follows:

$$\psi^\mu(z_e,z_h,\rho)=\frac{1}{\sqrt{N_z}}\sum_{n,m} B^\mu_{m,\gamma}\Phi^\gamma_m(z_e-nd,z_h-nd,\rho), \tag{32}$$

where

$$\Phi^\gamma_m(z_e,z_h,\rho)\equiv\varphi^\gamma_m(\rho)f^e(z_e-md)f^h(z_h) \tag{33}$$

is a two-well exciton state. The state $\Phi^\gamma_m(z_e,z_h,\rho)$ is an approximate eigenstate of a two-well Hamiltonian which only includes the band-edge potential for the hole well at $z_h=0$ and the electron well at $z_e=md$ along with the electron-hole Coulomb interaction.[14] The quantum number γ (which could be $1s,2p$, etc.) is the in-plane excitation quantum number for the two-well eigenstate. The functions $f^e(z_e)$ and $f^h(z_h)$ are the single-particle electron and hole one-dimensional (1D) eigenstates, respectively, of isolated wells centered at $z=0$. In practice, the $\varphi^\gamma_m(\rho)$ are variational functions with variational parameters that are determined by minimizing the energy of the given two-well exciton Hamiltonian as described in Ref. 14. The functions $\varphi^\gamma_m(\rho)$ with the same m but different γ are orthogonal. Finally, the $B^\mu_{m,\gamma}$ are expansion coefficients determined by diagonalizing the full exciton Hamiltonian in the two-well basis.[14]

Using Eqs. (32) and (33) in Eq. (29), we obtain

$$\psi^\mu_m(\mathbf{k})=\sum_{n,p,\gamma} B^\mu_{p,\gamma}C^{e*}_{n+p-m}C^h_n\varphi^\gamma_p(\mathbf{k}), \tag{34}$$

where

$$\varphi^\gamma_p(\mathbf{k})\equiv\frac{1}{\sqrt{A}}\int d^2\rho\,\varphi^\gamma_p(\rho)e^{i\mathbf{k}\cdot\rho}, \tag{35}$$

and the $C^{e,h}_n$ are the expansion coefficients employed in Eqs. (3) and (4), but where the expansion is in terms of the tight-binding single-well states, $f^{e,h}(z_{e,h})$, rather than in terms of Wannier states. Despite the use of tight-binding states, the calculation is still done beyond the nearest-neighbor approximation.

By using Eq. (34) in Eq. (31) and employing the summation rules for the $C^{e,h}_n$ found in the Appendix along with the orthonormality of the $\varphi^\gamma_m(\rho)$, Eq. (31) reduces to

$$i\hbar\frac{dD_\nu}{dt}=-\frac{i\hbar}{T_2}D_\nu+\mathbf{M}^\nu\cdot\boldsymbol{\mathcal{E}}_o(t)e^{i\omega_\nu t}+eF(t)d$$
$$\times\sum_\mu D_\mu e^{-i(\omega_\mu-\omega_\nu)t}\sum_m m\sum_\gamma B^{\nu *}_{m,\gamma}B^\mu_{m,\gamma}, \tag{36}$$

where the optical transition matrix is given by

$$\mathbf{M}^\nu\equiv\frac{1}{\sqrt{A}}\sum_m \mathbf{d}^{cv}_{-m}\sum_{\mathbf{k}} \psi^{\nu *}_m(\mathbf{k}) \tag{37}$$

$$=\mathbf{M}_o\frac{1}{\sqrt{N_z}}\int dz\,\psi^{\nu *}(z,z,0) \tag{38}$$

$$=\mathbf{M}_o\sum_m B^{\nu *}_{m,\gamma}\varphi^{\gamma *}_m(\rho=0)\int dz\, f^e(z-md)f^h(z). \tag{39}$$

It is important to note that $\mathbf{M}^\nu$ will be very small except for the subset of states for which there is appreciable electron-hole overlap. As a result, the states with $1s$-like motion are much more strongly coupled to the optical field than the states with higher-energy in-plane motion. Thus, to simplify the calculations, from now on we shall restrict ourselves to states with $1s$-like in-plane motion. It should be pointed out that in some situations the states of higher in-plane excitation can play an important role. These states are responsible for Fano resonances[32] and for high excitation densities can result in electron-exciton correlations. However, as this is the first calculation on this system, we shall only include the $1s$ states in the basis employed in this paper. As has been shown previously, the optical transition matrix will also only be appreciable for states for which the along-axis electron-hole separation is small,[14] this typically will be a set of only 10–20 states (even for very small F_o). Thus the equations of motion for D_ν is a relatively small set of coupled linear first-order differential equations which can easily be solved numerically using say a Runge-Kutta algorithm.

C. Polarization

Now that we have a set of equations for the coefficients $D_\nu(t)$, which can be solved numerically, it remains to write the expression for the polarization in terms of these. The full polarization is given by

$$\mathbf{P}(t)=\mathbf{P}_{inter}(t)+\mathbf{P}_{intra}(t), \tag{40}$$

where $\mathbf{P}_{inter}(t)$ and $\mathbf{P}_{intra}(t)$ are the interband and intraband components, respectively, of the polarization. The interband polarization is given by

$$\mathbf{P}_{inter}(t)=\frac{2}{Ad}\sum_{m}\ \mathrm{Re}\left\{\mathbf{d}_{-m}^{cv*}\sum_{\mathbf{k}}\ P_{m}(\mathbf{k})\right\}. \tag{41}$$

If we use Eq. (30), the first-order interband polarization in terms of the D_{ν} is given simply by

$$\mathbf{P}_{inter}^{(1)}(t)=-\frac{2}{d}\sum_{\nu}\ \mathrm{Re}\{\mathbf{M}^{\nu*}D_{\nu}(t)e^{-i\omega_{\nu}t}\}. \tag{42}$$

The intraband polarization is given by

$$\mathbf{P}_{intra}(t)=-\frac{\hat{\mathbf{e}}_{z}e}{AN_{z}d}\sum_{n,m}\sum_{\mathbf{k}}\ f^{e}(n,n+m,\mathbf{k})\times\int dz\chi_{n}^{e*}(z)z\chi_{n+m}^{e}(z) \tag{43}$$

$$-\frac{\hat{\mathbf{e}}_{z}e}{AN_{z}d}\sum_{n,m}\sum_{\mathbf{k}}\ f^{h}(n+m,n,\mathbf{k})\times\int dz\chi_{n}^{h*}(z)z\chi_{n+m}^{h}(z) \tag{44}$$

$$=\frac{2e\hat{\mathbf{e}}_{z}}{A\hbar\omega_{B}}\sum_{m>0}\sum_{\mathbf{k}}\ \mathrm{Re}[\varepsilon_{m}^{e}f_{m}^{e}(\mathbf{k})+\varepsilon_{m}^{h}f_{-m}^{h}(\mathbf{k})] \tag{45}$$

$$-\frac{e\hat{\mathbf{e}}_{z}}{AN_{z}}\sum_{n}\sum_{\mathbf{k}}\ [f^{e}(n,n,\mathbf{k})-f^{h}(n,n,\mathbf{k})]. \tag{46}$$

Somewhat surprisingly, the second set of terms in this expression do not sum to zero if the limit of an infinite system is taken only after the sum is performed. We now use the time-scale corrected coherent limit (TCCL) approximation of Axt, Bartels, and Stahl[11] to obtain the approximate relation

$$f^{e(2)}(n,n+m,\mathbf{k})=\sum_{n'}\ P^{(1)*}(n',n,k)P^{(1)}\times(n',n+m,k)e^{[(2/T_{2})-(1/T_{1})]t} \tag{47}$$

and a similar relation for the holes. Using this in Eq. (45) and employing summation relations found in the Appendix we obtain

$$\mathbf{P}_{intra}^{(2)}(t)=\frac{2e\hat{\mathbf{e}}_{z}}{A\hbar\omega_{B}}\sum_{m>0}\sum_{\mathbf{k}}\ \mathrm{Re}[\varepsilon_{m}^{e}f_{m}^{e(2)}(\mathbf{k})+\varepsilon_{m}^{h}f_{-m}^{h(2)}(\mathbf{k})] \tag{48}$$

$$-\frac{e\hat{\mathbf{e}}_{z}}{A}e^{[(2/T_{2})-(1/T_{1})]t}\sum_{m}\ m\sum_{\mathbf{k}}\ |P_{m}^{(1)}(\mathbf{k})|^{2} \tag{49}$$

$$=-e\hat{\mathbf{e}}_{z}e^{[(2/T_{2})-(1/T_{1})]t}\sum_{\nu,\mu}\ D_{\nu}^{(1)*}(t)D_{\mu}^{(1)}(t)\times e^{-i(\omega_{\mu}-\omega_{\nu})t}\sum_{m}\ m\sum_{\gamma}\ B_{m,\gamma}^{\nu*}B_{m,\gamma}^{\mu}. \tag{50}$$

It can easily be seen that this expression contains both the dc polarization as well as the terahertz contributions.[33]

The primary quantity of interest in this work is the spectrally resolved linear absorption of the optical pulse. If we make the common assumption that the propagation distance L is much less than the wavelength of the light, and that the polarization is approximately spatially constant we get the following expression for the absorption coefficient:[34]

$$\alpha(\omega)\equiv-\frac{I(L,\omega)-I(0,\omega)}{I(0,\omega)L} \tag{51}$$

$$=B\frac{\mathrm{Im}\{\mathbf{P}_{inter}^{(1)}(\omega)\mathbf{A}^{*}(\omega)\}}{|\mathbf{A}(\omega)|^{2}}, \tag{52}$$

where

$$B\equiv\frac{4\pi\omega_{c}^{2}}{\kappa c^{2}}, \tag{53}$$

$$\mathbf{A}(\omega)=\int_{-\infty}^{\infty}\boldsymbol{\mathcal{E}}_{o}(t)e^{-i(\omega-\omega_{c})t}dt, \tag{54}$$

and

$$\mathbf{P}_{inter}^{(1)}(\omega)=\int_{-\infty}^{\infty}\mathbf{P}_{inter}^{(1)}(t)e^{-i(\omega-\omega_{c})t}dt, \tag{55}$$

where ω_{c} is the central frequency of the laser pulse.

We note that a more accurate evaluation of the absorption spectrum requires a spatially dependent polarization. If the pulse wave vector is parallel to the growth axis z, then we have to allow for spatial variation in the z direction. This can be accomplished by including all of the interband density-matrix elements $P(m_{1},m_{2},\mathbf{k})$, not just those of the form $P(0,m,\mathbf{k})$. This would increase the size of the problem by a factor of N_{b}, where N_{b} is the number of electronic or hole WSL basis states. However, because of the rapid convergence of this basis, N_{b} is relatively small ($\lesssim 30$) the problem would still be tractable. Such a calculation would likely be prohibitive in a k_{z}-state basis because of the large number of basis states required. For the purpose of this work we will perform the calculation assuming a spatially constant polarization.

III. RESULTS

The system we shall model in all of the following is a $GaAs/Ga_{0.6}Al_{0.3}As$ superlattice with well widths of 67 Å and barrier widths of 17 Å. This is the structure of the superlattice that was studied in the recent DFWM experiments of Bloch oscillations.[22,23] The physical parameters used to model the system (effective masses, band offsets, etc.) are the same as those employed in a number of earlier works.[14,22,23] The electron miniband width for this system is

approximately $\Delta_e = 38$ meV, while the heavy-hole miniband width is $\Delta_h = 3$ meV. The calculations are all done for a static electric field of $F_o = 15$ kV/cm. The terahertz field is taken to be monochromatic and of the form

$$F(t) = F\cos(\omega_F t + \phi). \tag{56}$$

Although existing sources of terahertz radiation typically produce pulses that are only a few cycles in duration, we have considered the problem of a CW terahertz source because it leads to conceptually simpler results while retaining the basic physics. For simplicity, we will present all angular frequencies in units of ω_B, and all times in units of $1/\omega_B$, where $\omega_B \equiv eF_o d/\hbar$ is the Bloch oscillation angular frequency. For the system considered here $1/\omega_B = 52.2$ fs. We take the sample to be optically excited by a Gaussian pulse with a central frequency given by the energy of the $n=0$ WSL state in the absence of a terahertz field. The choice of central frequency is relatively unimportant as the absorption results only depend weakly on the central frequency for a wide range of central frequencies. The form of the optical field is taken in the rotating wave approximation to be

$$\boldsymbol{\mathcal{E}}_o(t) = \mathbf{A}_o e^{-(t/\tau_p)^2} e^{-i\omega_c t}, \tag{57}$$

where $\tau_p = 0.5/\omega_B$, giving a temporal pulse width of approximately 31 fs. The absorption results are essentially independent of the temporal pulse width, as long as it is less than the BO period ($\simeq 328$ fs) as we shall discuss later. The pulse duration is chosen to be small to ensure the pulse width is much less than the BO period.

The numerical results are calculated a follows. First the $1s$-excitonic WSL states (without the terahertz field) are calculated by employing the method of Dignam and Sipe.[14] Then, the resulting set of coupled first-order differential equations [Eq. (36)] are solved using a fifth-order Runge-Kutta algorithm, employing the B_m^μ and ω_μ found in the first step. The $D_\nu(t)$ are solved for times ranging from just before the optical pulse arrives until the interband polarization has essentially completely dephased ($t \simeq 20T_2$). The $D_\nu(t)$ are then used in Eq. (42) to calculate the interband polarization. Finally, we take a fast Fourier transform (FFT) of $\mathbf{P}^{(1)}_{inter}(t)$ to calculate the absorption spectrum via Eq. (52). Because the excitonic WSL states need only be recalculated when the structure or the static electric field is changed, the method is extremely fast when only the exciting pulse or the terahertz field characteristics are being changed. On a 200-MHz Pentium Pro, one spectrum can be calculated in less than 15 sec. In addition, the method is such that if $F(t)$ is simply a constant, F, the results obtained are exactly the same as would be obtained if F_o were replaced by $F_o + F$.

We begin by presenting in Fig. 1 the absorption spectrum in the absence of a terahertz field, calculated as described above for both $1s$ excitons and noninteracting electrons and holes (denoted by NI from now on) for an interband dephasing time of $T_2 = 10/\omega_B$.[35] The results in the NI case are for noninteracting, single-particle, $\mathbf{k}=0$ states with $\phi_p^\gamma(\mathbf{k}) = \delta_{\mathbf{k},0}\delta_{\gamma,0}$. In addition the NI results have been calculated in the nearest-neighbor tight-binding limit. The primary effect of this is that there is only coupling of adjacent WSL states via the terahertz field. The excitonic results are only for the $1s$-like excitons and have been calculated beyond the nearest-neighbor approximation. In both cases the laser frequency was centered at the $n=0$ state energy (which is different for the excitons and NI states due to the excitonic binding energy). Both absorption spectra are presented in arbitrary units. For both the NI and excitonic results, each absorption peak can be associated with a particular WSL state (NI or excitonic, respectively). For the static electric field strength chosen, there is a clear correspondence between the excitonic states and the usual NI WSL states. Thus, in all that follows, both the NI and EX states (and the absorption peaks associated with them) shall be labeled by the index n, which gives the approximate average separation of the electrons and holes in the z direction in units of d (i.e., the usual WSL index).

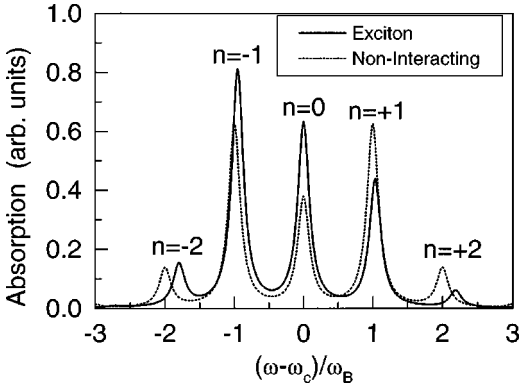

FIG. 1. The calculated absorption as a function of frequency for excitons (solid) and for the model of noninteracting (NI) electrons and holes (dashed) for the superlattice structure with a static electric field of $F_o = 15$ kV/cm without a terahertz field. The interband dephasing time is taken to be $T_2 = 10/\omega_B$. The frequency is referenced to the $n=0$ NI WSL state energy for the NI results and to the $n=0$ excitonic state for the excitonic results. As a result, the actual excitonic binding energies of the states cannot be obtained from this plot. The *differences* in binding energies, however, are evident in the different spacings between the excitonic peaks.

The results show the basic features that have been well explained in previous publications.[14] The NI spectra is symmetric about the $n=0$ state with equal frequency spacings of ω_B between states. Although it not clearly evident here, due to the centering of the spectra on the $n=0$ states, the peak associated with each excitonic state is shifted down in energy relative to the NI peaks by the electron-hole binding energy of that state. The states with smallest n values are shifted the most, as the binding energy is largest for these. In addition, the states with negative values of n are shifted more than those with positive values due to the strong mixing of $n<0$ states with the $n=0$ WSL state.[14] The important consequence of this is that *the excitonic WSL energy spacings are not equal*. When the terahertz field is included, the unequal energy-level spacings and the absorption asymmetry between $n>0$ and $n<0$ excitonic states yields much more complicated results for the excitonic spectra compared to the NI spectra. For this reason, we begin by presenting the results for the noninteracting case and will consider the excitonic case towards the end of this section.

A. Noninteracting electron-hole results

In Fig. 2 we present NI absorption spectra for a terahertz field with a frequency equal to the BO frequency ω_B. The

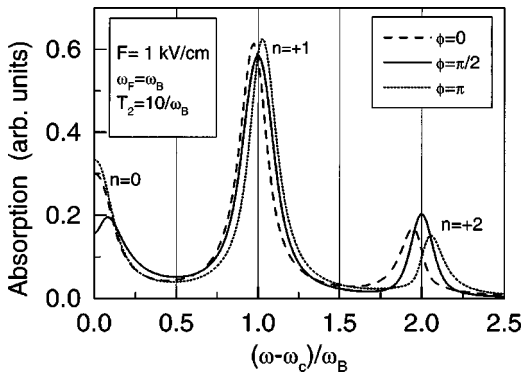

FIG. 2. The calculated NI absorption spectra for a static electric field of $F_o=15$ kV/cm and a terahertz field of amplitude $F=1$ kV/cm and frequency $\omega_F=\omega_B$. The interband dephasing time is $T_2=10/\omega_B$. The spectra are plotted for three different values of the terahertz phase: $\phi=0$ (dashed), $\phi=\pi/2$ (solid), and $\phi=\pi$ (dotted). The spectra obey the symmetry $\alpha(-(\omega-\omega_c))=\alpha(\omega-\omega_c)$, and so are only plotted for $\omega>\omega_c$.

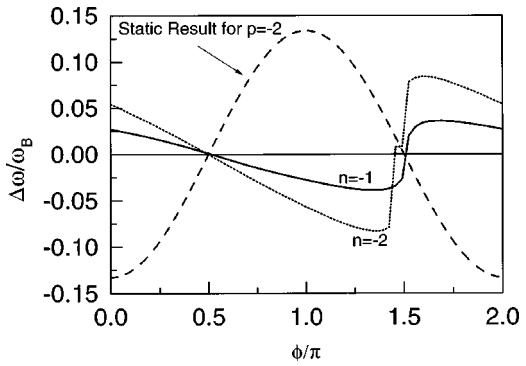

FIG. 3. The frequency shifts $\Delta\omega$ of the NI absorption peaks (relative to the peaks for no terahertz field) as a function of terahertz phase, ϕ, for a static electric field of $F_o=15$ kV/cm and a terahertz field of amplitude $F=1$ kV/cm and frequency $\omega_F=\omega_B$. The plotted curves are for the WSL states with $n=-1$ (solid) and $n=-2$ (dotted). The interband dephasing time is $T_2=10/\omega_B$. The $n=0$ curve is not included because the value is always zero. The $n<0$ curves are not plotted because they are identically the negative of the corresponding $n>0$ curves. The static result ($\omega_F=0$) for the $n=-2$ state is also shown as a dashed line for comparison.

interband dephasing time is chosen to be $T_2=10/\omega_B$. The spectrum is plotted for three different values of the terahertz phase, ϕ. The terahertz field is chosen to have a frequency equal to ω_B and an amplitude of 1 kV/cm because these are approximately the expected values for the terahertz field that would be generated by the Bloch-oscillating carriers in a pump-probe or DFWM experiment.[22,23] Because the spectra are symmetric under inversion about $\omega=\omega_c$, the results have only been plotted for $\omega>\omega_c$.[36] From Fig. 2 we see that the absorption peaks are closer together when $\phi=0$, unshifted when $\phi=\pi/2$, and further apart when $\phi=\pi$. This is precisely the opposite to what is predicted in the quasistatic model, where, for $\phi=0$, the instantaneous terahertz field at pulse center adds to the static field and the absorption peaks thus become further apart. In addition to the shifts, we also find a strong dip in the $n=0$ absorption peak at $\omega=\omega_c$ for $\phi=\pi/2$. These two features indicate that the quasistatic picture discussed in the Introduction is not valid here.

To display the absorption peaks shifts more clearly, we examine $\Delta\omega$, which is defined as the frequency shift of the peaks relative to the peaks calculated when $F=0$. In Fig. 3 we plot $\Delta\omega$ for the same conditions as in Fig. 2 as a function of terahertz phase ϕ for the $n=-2$ and $n=-1$ WSL states. We have not plotted the shift of the $n=0$ state because its centroid remains unchanged even when it splits into two peaks. The shifts change roughly sinusoidally with the phase and the maximum shift for the $n=-2$ state is approximately twice that for the $n=-1$ state. This all agrees with the ''quasistatic picture,'' where the terahertz field can be treated as a static field with a magnitude given by the value of the field at pulse center. However, the precise magnitude of the shifts is not simply given by $eF(t_o)nd$ and the sign of the shifts for a given phase ϕ is opposite to that predicted in the quasistatic picture. This can be seen by comparison of the curve for the $n=-2$ state with the results for the $n=-2$ state in the static ($\omega_F=0$) case (long dash). In fact, the calculated range of the frequency shift for the $n=-2$ state is only 63% of the range found in the static case and the curves are almost π out of phase.

The source of the above-mentioned discrepancies are illuminated by plotting the range of the peak shifts for each of the peaks as a function of the terahertz frequency ω_F for different values of the dephasing time (see Fig. 4). The range for a given WSL peak is defined as the maximum central frequency of a given peak minus the minimum frequency for terahertz phases over the range $\phi=[0,2\pi]$. At $\omega_F=0$ we have the amplitude of the static shift. As the terahertz frequency is increased, the shift amplitude decreases with the decrease being more rapid when T_2 is large. The physical origin of this effect is illustrated schematically in Fig. 5 and can be explained as follows. In all cases, T_2 is much larger than the optical pulse width. Thus, the time during which the optical electric field interacts with the terahertz field through the superlattice medium is given approximately by T_2, the time during which there is a significant interband polarization. If T_2 is much less than the terahertz period, $\tau_F \equiv 2\pi/\omega_F$, then the terahertz field does not change much over the duration of the interband polarization and the qua-

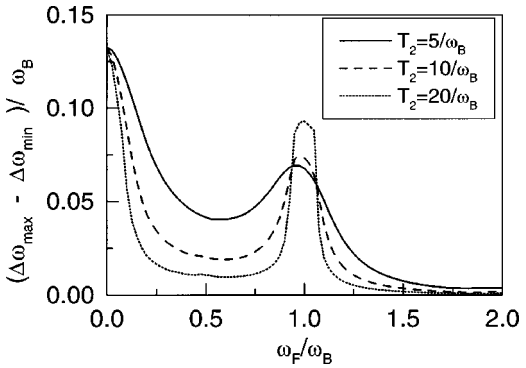

FIG. 4. The calculated range of frequency shifts of the NI absorption peaks as a function of the terahertz field frequency for a static electric field of $F_o=15$ kV/cm and a terahertz field of amplitude $F=1$ kV/cm. The three curves are for different values of the interband dephasing time: $T_2=5/\omega_B$ (solid), $T_2=10/\omega_B$ (dashed), and $T_2=20/\omega_B$ (dotted).

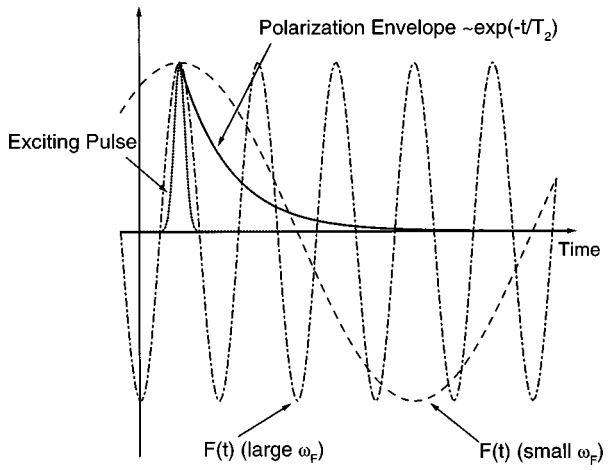

FIG. 5. A schematic plot demonstrating the physical mechanism behind the initial reduction in the frequency shifts of the absorption peaks as ω_F is increased from zero. The plot shows the exciting optical pulse envelope (dotted), the induced interband polarization envelope (solid), and two different terahertz fields. One is a relatively low-frequency field (dashed), while the other is much higher in frequency (dashed-dotted).

sistatic picture is valid. This is the case illustrated by the dashed line for $F(t)$ in Fig. 5. However, as ω_F increases, for a fixed T_2, the polarization begins to sample over a number of periods of the terahertz field, resulting in a reduction in the effective field amplitude, which should be used in the quasistatic model. This is the case illustrated by the dashed-dot line for $F(t)$ in Fig. 5. Thus, it is the suitable average of the terahertz field over the lifetime of the interband polarization which determines the effective value for the quasistatic field. When $\tau_F \ll T_2$ the averaging is over many periods and the effect of the terahertz field is essentially washed out. This effect is seen in Fig. 4 where the peak shifts for all of the states decrease rapidly as ω_F increases from zero.

A simple analytic form for this small-ω_F behavior is given by integrating the terahertz field, weighted by the decay envelope of the interband polarization (assumed to be a simple exponential with time constant T_2). This predicts a peak-shift range given by

$$R(\omega_F, T_2) = \frac{R_o}{\sqrt{1+(\omega_F T_2)^2}}, \tag{58}$$

where R_o is the static shift. This gives qualitative agreement with the calculated results for small ω_F, but is clearly an oversimplification. It is important to note that it is the *dephasing time and not the incident pulse duration* that determines this washing out of the quasistatic picture. One can also show that for this simple model that the first zero that occurs in the range as a function of ϕ, moves from $\phi = \pi/2$ to $\phi = 0$ as $\omega_F T_2$ goes from zero to infinity. Thus, the phase shift in this model will never be close to the shift of π found in the full calculations when $\omega_F = \omega_B$.

As the terahertz frequency is increased further, the peak-shift range increases dramatically for all values of T_2, peaking near $\omega_F = \omega_B$. This clearly cannot be due to the quasistatic mechanism mentioned above, as the terahertz period is much shorter than the dephasing time, and the sign of the

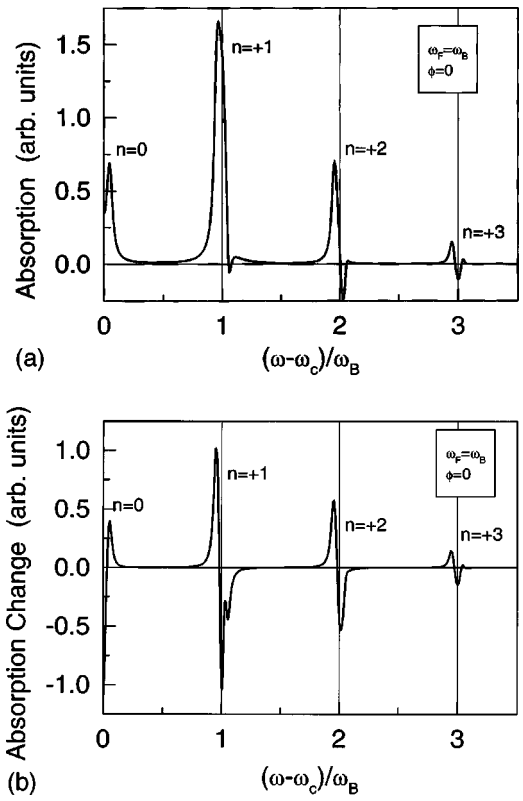

FIG. 6. (a) The calculated NI absorption spectra for a static electric field of $F_o = 15$ kV/cm and a terahertz field of amplitude $F = 1$ kV/cm, phase $\phi = 0$, and frequency $\omega_F = \omega_B$. The interband dephasing time is $T_2 = 40/\omega_B$. Note that for this value of the dephasing time there is optical gain over some ranges of the frequency. (b) The difference between the NI absorption spectra calculated in (a) and the spectra calculated with no terahertz field.

shifts is inconsistent with the quasistatic picture as discussed above. This range increase is the result of the terahertz field being resonant with transitions between all WSL states when $\omega_F = \omega_B$. One might expect, however, that the change in the absorption would be reflected as resonant mixing of the optical field with the terahertz field, which would not necessarily result in peak shifts, but rather in new peaks altogether.

To see how the resonant condition results in such large peak shifts, we present, in Fig. 6(a), the NI absorption spectrum for $\omega_F = \omega_B$, $F = 1$ kV/cm, $\phi = 0$, and $T_2 = 40/\omega_B$. Comparing these results with those presented in Fig. 1, we see that not only are the absorption peaks narrower due to the longer dephasing time (as expected), but there are actually *frequency ranges where there is gain*. The regions of gain can be understood as the result of nonlinear sum and difference mixing of the optical and the terahertz frequencies. The relative phase of the nonlinear polarization and the electric field of the incident optical pulse determines whether there is constructive or destructive interference, and hence whether there is gain or absorption. There are no regions of gain observed for the results when $T_2 = 10/\omega_B$ (see Fig. 2) due to the peak broadening associated with the more rapid dephasing, thus is it not clear whether this gain would be seen in experiments where the dephasing time is typically 1 ps ($\sim 20/\omega_B$). The origin of the peak shifts can clearly seen in Fig. 6(b) where we plot the difference between the absorption spectrum plotted in Fig. 6(a) and the spectrum obtained

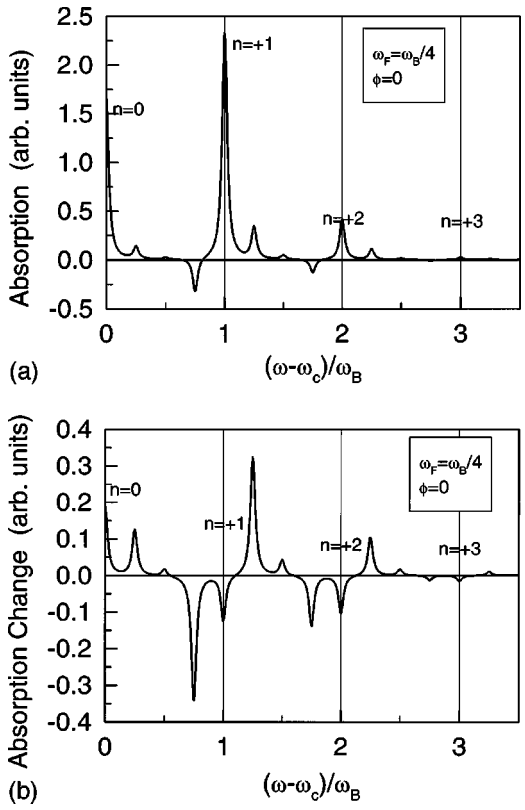

FIG. 7. (a) The calculated NI absorption spectra for a static electric field of $F_o=15$ kV/cm and a terahertz field of amplitude $F=1$ kV/cm, phase $\phi=0$, and frequency $\omega_F=\omega_B/4$. The interband dephasing time is $T_2=40/\omega_B$. Note that there is optical gain at $\omega_F=\omega_c\pm(m+\frac{3}{4})\omega_B$ where $m=\{0,1,2\}$. (b) The difference between the NI absorption spectra calculated in (a) and the spectra calculated with no terahertz field.

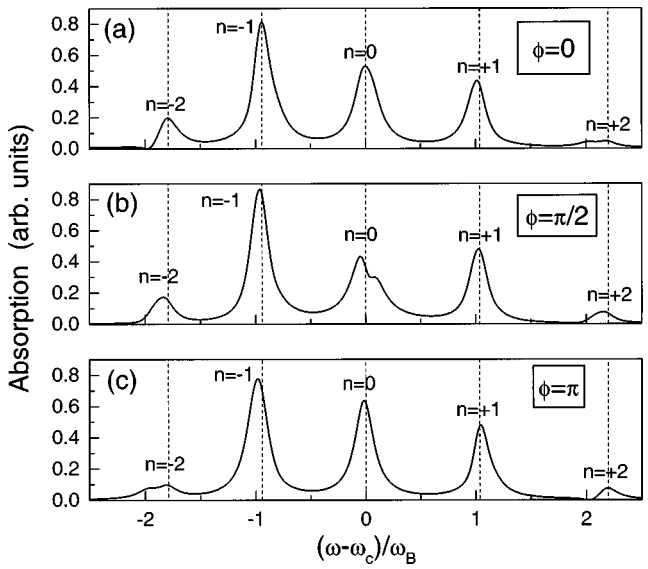

FIG. 8. The calculated excitonic absorption spectra for a static electric field of $F_o=15$ kV/cm and a terahertz field of amplitude $F=1$ kV/cm and frequency $\omega_F=\omega_B$. The interband dephasing time is $T_2=10/\omega_B$. The spectra are plotted for three different values of the terahertz phase: $\phi=0$ (a), $\phi=\pi/2$ (b), and $\phi=\pi$ (c). The vertical dashed lines indicate the centers of the excitonic absorption peaks in the absence of a terahertz field.

for $F=0$. This plot shows the resonancelike structure as the frequency is swept past each of the $F=0$ absorption peaks. The peaks shift in frequency due to the additional absorption on one side of the original peak and the gain on the other. This effect is even more clearly seen in Fig. 7, where the absorption spectrum has been plotted for the same configuration as in Fig. 6 except that $\omega_F=\omega_B/4$ (rather than $\omega_F=\omega_B$). Here the peaks and dips can be clearly located at frequencies $\pm\omega_B/4$ on either side of each $F=0$ absorption peak. In addition, peaks are found midway between the WSL absorption peaks due to higher-order nonlinearity. All of these peaks are due to nonlinear mixing of the optical frequencies with the terahertz frequency. Thus, in the case where $\omega_F=\omega_B$ the sum and difference frequency generation is acting in a way that gives results similar to those found in the $\omega_F=0$ case but the mechanism is very different.

The results for $\omega_F=\omega_B$ are qualitatively the same for terahertz field amplitudes other than $F=1$ kV/cm unless the field is so strong that the resonantlike structures arising from different peaks begin to interfere with each other. For the system considered here, this becomes a serious consideration for fields above 3 kV/cm. From the field dependence of the shift ranges (not shown), one finds a nearly linear increase in the ranges for each of the states up to about 1.2 kV/cm, with the shift ranges for the $n=\pm2$ states being essentially twice that of the $n=\pm1$ states as expected. However, above this field, the $n=\pm1$ state shift ranges increase more rapidly with field, such that for a field of $F=3$ kV/cm, the shifts for the $n=\pm2$ states are less than 1.5 times that of the $n=\pm1$ states. For higher fields still, the rate of change in the shift range with F is approximately the same for all of these states, again showing a marked deviation from the quasistatic model.

B. Excitonic results

In this section we present results of absorption calculations for $1s$-like excitons. Some of the features of the excitonic results are similar to the NI results but they are more complicated due to the unequal level spacings and mixing between the different NI WSL states that results from the electron-hole Coulomb interaction.

In Fig. 8 we present the excitonic absorption spectra for a terahertz field amplitude of 1 kV/cm and frequency equal to the BO frequency. The interband dephasing time employed is $T_2=10/\omega_B$ and the spectrum is plotted for three different values of the terahertz phase, ϕ. As can be seen, the absorption peaks are shifted as they were in the NI results, with the amount of shift depending upon the peak index and the terahertz phase. However, the sign and magnitude of the shifts are not the same as were found in the NI case. In addition, a number of the peaks ($n=+2$ for $\phi=0$ and $n=-2$ for $\phi=\pi$) are split into two peaks by the terahertz field. Both of these effects are essentially due to the fact that the terahertz frequency is not equal to the spacings between the excitonic states. Because of the unequal level spacing, the resonantlike responses seen in Fig. 6(b) do not fall right on top of the $F=0$ absorption peaks, and hence nature of the peak shifting is changed. By choosing the terahertz frequency to be resonant with the energy spacings between two particular exci-

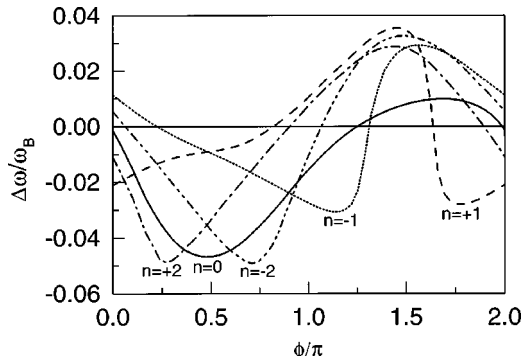

FIG. 9. The calculated frequency shifts $\Delta\omega$ of the excitonic absorption peaks (relative to the peaks for no terahertz field) as a function of terahertz phase ϕ for a static electric field of $F_o = 15$ kV/cm and a terahertz field of amplitude $F = 1$ kV/cm and frequency $\omega_F = \omega_B$. The plotted curves are for the states with $n = -2$ (dash-dot-dot), $n = -1$ (dotted), $n = 0$ (solid), $n = +1$ (dashed), and $n = +2$ (dash-dot). The interband dephasing time is $T_2 = 10/\omega_B$.

tonic states, one could increase the shift of at least one of those two states. However, in general the terahertz field would still not be resonant with any other transitions, and shifts for *those* states would not likely increase much and some would even decrease.

In Fig. 9 we present the frequency shifts of the excitonic peaks relative to the $F = 0$ results, as a function of terahertz phase, ϕ, for the first few excitonic states. For the peaks that split into two, for simplicity we have considered only the position of the highest peaks. The results are qualitatively similar to the NI results shown in Fig. 3 except that the symmetry of the positive and negative n states no longer exists, and the $n = 0$ state experiences a shift (which it did not in the NI case). These differences are due to the mixing of the NI WSL states via the electron-hole Coulomb interaction.

In Fig. 10 we plot the range of the peak shifts for the $n = -1,0,1$ excitonic states as a function of the terahertz frequency for different values of the dephasing time. Again the behavior is qualitatively similar to the NI results. In particular, the peak shift range decreases from its value at $\omega_F = 0$, and then peaks again near $\omega_F = \omega_B$. The frequencies at which the range is a maximum for the $n = -1$ and $n = +1$ states are found to be very nearly equal to the frequency separation of these states from the $n = 0$ state ($= 0.95\omega_B$ for $n = -1$ and $= 1.04\omega_B$ for $n = +1$). This is to be expected, since this is the condition for resonant coupling of these states to the $n = 0$ state via the terahertz field. The coupling of the $n = \pm 1$ states to the $n = \pm 2$ states is relatively unimportant because the optical oscillator strength of these states is much lower than that of the $n = 0$ state. Somewhat surprisingly, for the $n = 0$ state the range is greater near $\omega_F = \omega_B$ than at $\omega_F = 0$. We finally note that there is a small resonance in the amplitude for the $n = 0$ state near $\omega_F = 1.8\omega_B$. This is due to the small coupling between the $n = 0$ and $n = -2$ states via the terahertz field. This was not seen in the NI results because it is forbidden in the nearest-neighbor tight-binding model that we employed in the NI calculations.

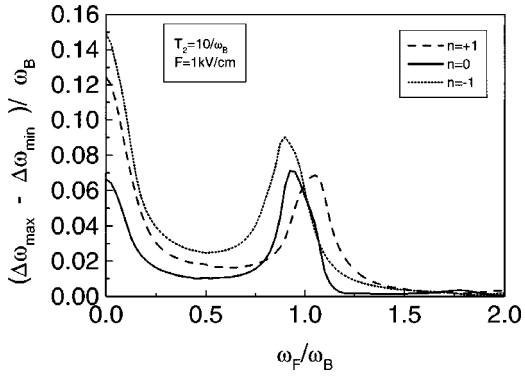

FIG. 10. The calculated range of frequency shifts of the excitonic absorption peaks as a function of the terahertz field frequency for a static electric field of $F_o = 15$ kV/cm, an interband dephasing time of $T_2 = 10/\omega_B$, and a terahertz field of amplitude $F = 1$ kV/cm. The plotted curves are for the states with $n = -1$ (dotted), $n = 0$ (solid), and $n = +1$ (dashed).

It is perhaps surprising that the excitonic results are even qualitatively similar to the NI results when $\omega_F = \omega_B$, given that the terahertz frequency is no longer resonant with the excitonic state-energy separations. This result is partially due to the fact that the static field is large enough such that excitonic binding energies are less that the WSL energy spacings. In this case terahertz fields can be found that are nearly resonant with a number of the excitonic WSL transitions. We find in contrast that the excitonic results for large period superlattices, or superlattices in small static electric fields often bear little resemblance to the NI results.

IV. CONCLUSION

We have presented the results of a calculation of the absorption spectra of a semiconductor superlattice in an along-axis time-dependent electric field. The method used is based upon a form of the SBE's that employ a basis of noninteracting electron and hole WSL states rather than the usual k_z-state basis. We find that the resulting equations are particularly simple when a basis of two-well exciton states are employed in formulation of the solution. The original motivation of this calculation was to try to understand the results of recent DFWM experiments, where in a mean-field approximation the terahertz field can be considered to be generated by the Bloch-oscillating carriers excited by the pump pulse. The results presented in this work, however, are also of interest in their own right, as it is certainly technically feasible to apply an external terahertz field to a superlattice.

The calculations presented show that for low enough frequencies of the terahertz field, the excitonic absorption peaks shift with the phase of the terahertz field as if they are responding to the instantaneous terahertz field at optical pulse center. However, for frequencies near the Bloch oscillation frequency ω_B we find that the shifts can be thought of as that resulting from the frequency mixing between the optical and terahertz fields. Because this effect relies to a large degree on the WSL energy spacing being equal to the terahertz photon energy, the shifts can be quite different when excitonic effects are included than when the Coulomb interaction between the electrons and holes is neglected. Despite this, the same basic effect is found for the excitonic levels as long as the static electric field is strong enough such that WSL en-

ergy spacings are greater than the excitonic binding energies. We also found that, for terahertz frequencies that differ from 0 or ω_B by more than the inverse of the interband dephasing time, there is only a weak shifting of the absorption peaks by the terahertz field.

As is stands, this work is not directly applicable to DFWM experiments.[22,23] However, the absorption peak shifts calculated in this work agree qualitatively with the experimentally observed peak shifts in the DFWM experiments. This suggests that the peak shifts in these experiments may be due to frequency mixing of optical and terahertz fields, where the terahertz field is generated by the Bloch oscillating carriers. This is different from the quasistatic picture that was originally presented in the above-mentioned papers. However, this does not likely affect the basic results or conclusions presented in those papers, as the difference in amplitude predicted by the two interpretations is within experimental error and the phase of the shifts cannot be simply compared. To more definitively determine the source and nature of the peaks shifts requires a complete calculation of the third-order intraband polarization for DFWM experiments. The formalism presented in this work is very well suited to tackling this problem and we are currently pursuing it. Finally, in this work we have only included $1s$-like excitons in the calculation. Although many experiments and theoretical studies indicate that the $1s$ excitons are the most important component in linear absorption,[14] DFWM,[5] and terahertz emission,[11] states of higher in-plane motion should be included in future calculations of DFWM spectra, as these higher-energy states will undoubtedly play a significant role.

ACKNOWLEDGMENTS

I would like to thank Karl Leo for bringing this subject to my attention and Margaret Hawton, Karl Leo, and John Sipe for valuable discussions related to this topic. This work was supported in part by the Natural Sciences and Engineering Research Council of Canada.

APPENDIX: PROPERTIES OF THE WANNIER-STARK LADDER EXPANSION COEFFICIENTS

In this appendix we present some important relations for the expansion coefficients C_m^e for the WSL states and some of the consequences of these relations.

In Eq. (3) we have neglected coupling between different minibands via the static electric field (i.e., Zener tunneling) and given the following expansion of the WSL states for the electrons in terms of Wannier states of the lowest conduction miniband:

$$\chi_n^e(z)=\sum_m C_{m-n}^e a^c(z-md). \tag{A1}$$

It can be shown that, within this one-band model, if the superlattice potential has inversion symmetry in the z direction, the expansion coefficients are given exactly by

$$C_m^e=\frac{1}{N_z}\sum_{k_z} \exp\left\{ i\left[mk_z d+\frac{1}{eF_o}\int_0^{k_z} dk(\epsilon^e(k)-\varepsilon_0^e)\right]\right\}. \tag{A2}$$

In the nearest-neighbor tight-binding limit, the above expression reduces to the usual form, $C_m^e=J_m(\theta_e)$, where $\theta_e \equiv \Delta_e/(2eF_o d)$.

Using Eq. (A2) and the corresponding equation for C_m^h, we can derive the following relation between the intraband and interband density matrix elements present here and those found in the usual k_z-state basis:

$$f_m^e(\mathbf{k})=\frac{1}{N_z}\sum_{k_z} n_e(k_z,\mathbf{k})e^{imk_z d}, \tag{A3}$$

$$P_m(\mathbf{k})=\frac{1}{N_z}\sum_{k_z} \exp\left\{ i\left[mk_z d-\frac{1}{eF_o}\int_0^{k_z} dk(\epsilon^e(k)-\varepsilon_0^e - \epsilon^h(k)+\varepsilon_0^h)\right]\right\} P(k_z,\mathbf{k}), \tag{A4}$$

where $n_e(k_z,\mathbf{k})$ and $P(k_z,\mathbf{k})$ are the intraband and interband density matrices, respectively, in the k_z-space basis.[4] These expressions are fully invertible; thus when the z_p^λ are zero there is a one-to-one correspondence between the density matrices in the two bases. The primary advantages of the WSL basis is the transparency of the results, and the ease of calculation. From Eq. (A3), it is clear that $f_0^e(\mathbf{k})$ gives the average population of all the electron states with the in-plane wave vector $\mathbf{k}$.

Using Eq. (A2), we can also derive the following summation relations for the expansion coefficients:

$$\sum_n C_n^{e*} C_{n+p}^e=\delta_{p,0}, \tag{A5}$$

$$\sum_n nC_n^{e*} C_{n+p}^e=\frac{-1}{eF_o d}[\varepsilon_p^e-\delta_{p,0}\varepsilon_0^e]. \tag{A6}$$

These have been used in deriving a number of the equations in the theory section, and can easily be verified in the nearest-neighbor tight-binding limit.

Directly analogous relations can also be found for the hole states.

[1] K. Leo, T. C. Damen, J. Shah, E. O. Göbel, and K. Köhler, Appl. Phys. Lett. **57**, 19 (1990).

[2] K. Leo, J. Shah, E. O. Göbel, T. C. Damen, S. Schmitt-Rink, W. Schäfer, and K. Köhler, Phys. Rev. Lett. **66**, 201 (1991).

[3] J. Feldmann, K. Leo, J. Shah, D. A. B. Miller, J. E. Cunningham, T. Meier, G. von Plessen, A. Schulze, P. Thomas, and S. Schmitt-Rink, Phys. Rev. B **46**, 7252 (1992).

[4] See, e.g., H. Haug and S. W. Koch, *Quantum Theory of the Optical and Electronic Properties of Semiconductors*, 3rd ed. (World Scientific, Singapore, 1994).

[5] Jörg Hader, Torsten Meier, Stephan W. Koch, Fausto Rossi, and Norbert Linder, Phys. Rev. B **55**, 13 799 (1997).

[6] T. Meier, G. von Plessen, P. Thomas, and S. W. Koch, Phys. Rev. Lett. **73**, 902 (1994).

[7] T. Meier, G. von Plessen, P. Thomas, and S. W. Koch, Phys. Rev. B **51**, 14 490 (1995).

[8] T. Meier, F. Rossi, P. Thomas, and S. W. Koch, Phys. Rev. Lett. **75**, 2558 (1995).
[9] T. Meier *et al.*, Phys. Low-Dimens. Semicond. Struct. **3/4**, 1 (1998).
[10] K. Victor, V. M. Axt, and A. Stahl, Phys. Rev. B **51**, 14 164 (1995).
[11] V. M. Axt, G. Bartels, and A. Stahl, Phys. Rev. Lett. **76**, 2543 (1996).
[12] Margaret Hawton and Delene Nelson, Phys. Rev. B **57**, 4000 (1998).
[13] E. E. Mendez, F. Agulló-Rueda, and J. M. Hong, Phys. Rev. Lett. **60**, 2426 (1988).
[14] M. M. Dignam and J. E. Sipe, Phys. Rev. Lett. **64**, 1797 (1991); M. M. Dignam and J. E. Sipe, Phys. Rev. B **43**, 4097 (1991).
[15] M. Dignam, J. E. Sipe, and J. Shah, Phys. Rev. B **49**, 10 502 (1994).
[16] D. M. Whittaker, Phys. Rev. B **41**, 3238 (1990); D. M. Whittaker *et al.*, *ibid.* **41**, 3238 (1990).
[17] See, e.g., Dignam, Sipe, and Shah (Ref. 15) and references therein.
[18] C. Waschke, H. G. Roskos, R. Schwedler, K. Leo, H. Kurz, and K. Köhler, Phys. Rev. Lett. **70**, 3319 (1993).
[19] G. von Plessen and P. Thomas, Phys. Rev. B **45**, 9185 (1992).
[20] Norbert Linder, W. Geisselbrecht, G. Philipp, K. H. Schmidt, and G. H. Döhler, J. Phys. IV **3**, C-195 (1993); Norbert Linder, Klaus H. Schmidt, Wolfgang Geisselbrecht, Gottfried H. Döhler, Hogler T. Grahn, Klaus Ploog, and Harald Schneider, Phys. Rev. B **52**, 17 352 (1995).
[21] A. M. Bouchard and M. Luban, Phys. Rev. B **47**, 6815 (1993).
[22] M. Sudzius, V. G. Lyssenko, F. Löser, K. Leo, M. M. Dignam, and K. Köhler, Phys. Rev. B **57**, R12 693 (1998).
[23] V. G. Lyssenko, G. Valušis, F. Löser, T. Hasche, K. Leo, M. M. Dignam, and K. Köhler, Phys. Rev. Lett. **79**, 301 (1997).
[24] Kristinn Johnsen and Antti-Pekka Jauho, Phys. Rev. B **57**, 8860 (1998).
[25] See, e.g., W. Schäfer, D. S. Kim, J. Shah, T. C. Damen, J. E. Cunningham, K. W. Goossen, L. N. Pfeiffer, and K. Köhler, Phys. Rev. B **53**, 16 429 (1998); G. Bartels, G. C. Cho, T. Dekorsy, H. Kurz, A. Stahl, and K. Köhler, *ibid.* **55**, 16 404 (1997).
[26] It should be noted that, because there is a one-to-one correspondence between the density-matrix elements in the two methods (see the Appendix), the physical content of the formalism in the two basis is the same. This has been pointed out previously by Hader *et al.* in Ref. 5.
[27] Paula Feuer, Phys. Rev. **88**, 92 (1952).
[28] The fact that elements such as $P(n+m,n,\mathbf{k})$ do not depend on n is a consequence of two factors: (1) The full excitonic Hamiltonian (including static and terahertz fields) is invariant under simultaneous translation of the exciton center of mass by an integral number of superlattice periods d in the z direction and (2) there are equal numbers of electrons and holes in the system. As a result of this, one can also show that any four-operator expectation values of the form $\langle \alpha^{\dagger}_{n+m_1,\mathbf{k}_1+\mathbf{q}} \beta^{\dagger}_{n+m_2,\mathbf{k}_2-\mathbf{q}} \beta_{n+m_3,\mathbf{k}_2} \alpha_{n+m_2,\mathbf{k}_1} \rangle$ are also independent of n.
[29] P. H. Bolivar, F. Wolter, A. Müller, H. G. Roskos, H. Kurz, and K. Köhler, Phys. Rev. Lett. **78**, 2232 (1997).
[30] Determining how to deal with the intraband dephasing constants is a nontrivial matter, as has been pointed out previously by other authors (Refs. 10, 11, and 29). There are approximate ways in which the problem can be dealt with in certain cases, such as the TCCL of Axt, Bartels, and Stahl (Ref. 11).
[31] M. M. Dignam and J. E. Sipe, Phys. Rev. B **45**, 6819 (1992).
[32] C. P. Holfeld, F. Löser, M. Sudzius, K. Leo, D. M. Whittaker, and K. Köhler, Phys. Rev. Lett. **81**, 874 (1998).
[33] In the absence of the electron-hole Coulomb interaction, it is easy to show that the sum over m given by $\Sigma_m m \Sigma_\gamma B^{\nu *}_{m,\gamma} B^{\mu}_{m,\gamma} = \nu \delta_{\nu,\mu} - (1/\hbar\omega_B)[\varepsilon^e_{\nu-\mu} + \varepsilon^h_{\nu-\mu} - \varepsilon^e_0 - \varepsilon^h_0]$. Thus the expression for the intraband polarization yields the dc polarization as well as the terahertz polarization associated with each harmonic of the superlattice dispersion relations.
[34] See, e.g., Y. R. Shen, *The Principles of Nonlinear Optics* (Wiley, New York, 1984), Chap. 3.
[35] For the system considered, this corresponds to a dephasing time of 0.52 ps. This time has been chosen to be somewhat smaller than the experimentally estimated dephasing time of 1 ps in order to aid in the discussion of the basic physical effects.
[36] It should be noted that one of the consequences of taking the central frequency to be different from the $n=0$ WSL state frequency would be to introduce a relatively weak asymmetry between the absorption for the $n>0$ and $n<0$ WSL states when $F \neq 0$. For simplicity we have not presented such cases in this paper.